JOURNAL OF CATALYSIS 85, 127–134 (1984)

Nitric Oxide Decomposition on Pt(410)

W. F. BANHOLZER[1] AND R. I. MASEL[2]

Department of Chemical Engineering, University of Illinois, 1209 W. California St., Urbana, Illinois 61801

Received April 28, 1983; revised August 4, 1983

The decomposition of nitric oxide on platinum (410) was studied by temperature-programmed desorption. The (410) surface was found to be unusually active for NO decomposition, decomposing more than 98% of the NO in the flash. Nitrogen desorption from an NO-covered Pt(410) surface was found to follow simple second-order kinetics, with an activation energy of 18 kcal/mol, and a preexponential (ν) of 3×10^{-3} cm^2/sec. The saturation coverage of NO at room temperature was found to be about half of that of CO on the same surface, suggesting that NO takes up two sites. These results show that $m(110) \times n(100)$ stepped surfaces with $n > m + 1$ are unusually active for NO bond breaking, as predicted by the orbital symmetry conservation model of W. F. Banholzer, Y. O. Park, K. M. Mak, and R. I. Masel (*Surf. Sci.* **128,** 176 (1983)).

INTRODUCTION

Previous workers have found that platinum is an active catalyst for nitric oxide decomposition. One of the anomalies in the data is that polycrystalline platinum samples are fairly active, but the single crystal samples studied so far have had limited activity. For example, Comrie *et al.* (*1*) studied NO desorption from a polycrystalline sample, which consisted mainly of (111) oriented crystallites, using temperature-programmed-desorption (TPD). They report that 75% of the NO which adsorbs on their sample at room temperature dissociates before it desorbs, where they calculate the percentage dissociation D, from

$$D = \frac{2P_{N_2}}{2P_{N_2} + P_{NO}} \qquad (1)$$

P_{N_2} in Eq. (1) is the N_2 TPD peak area, while P_{NO} is the NO TPD peak area. Similar measurements with a Pt(111) single crystal gives a D of less than 5% (*3–7, 13*). Pt(110) also shows little dissociation activity (*3, 8*). The (100) is catalytically active, but it gives a D of 50% under conditions where the polycrystalline sample gives a D of 75% (*3, 9–11, 24, 25*). Some work has been done with step surfaces, but all of the stepped surfaces considered previously gave D's of 50% or less (*6, 12, 13, 25*).

Woodward and Hoffmann (*14*) and Fukui (*15*) won a Nobel prize for showing that one can use the conservation of orbital symmetry to identify especially favorable reaction pathways in organic and inorganic systems. In their analysis, the formation and destruction of bonds during an elementary chemical reaction was viewed as a process where electrons are transferred from "donor" to "acceptor" orbitals. In some reactions, the donor and acceptor orbitals have the same symmetry, while in others they have a different symmetry. In the former case, a direct transfer of electrons is symmetry-allowed, while in the later case, a direct transfer is symmetry-forbidden. Hence the names "symmetry-allowed" and "symmetry-forbidden" for the two types of reactions.

In the last 20 years, there have been extensive studies of the effects of orbital symmetry on the rates of organic and inorganic reactions. It has been found (*14, 15, 28*) that there is generally an activation barrier associated with a symmetry constraint.

[1] Present address: General Electric Co., P.O. Box 8, Schenectady, N.Y. 12301.

[2] To whom correspondence should be addressed.

0021-9517/84 $3.00

Thus, reactions that are symmetry-allowed are usually favored over reactions that are symmetry-forbidden.

Recently we have considered whether arguments analogous to those above would yield useful insights into the plane to plane variations in activity for reactions on single crystal catalysts (*16*). A typical catalytic reaction consists of a series of elementary steps where bonds between the adsorbate and the catalyst are formed and destroyed. Each of these steps involved an electron transfer either into or out of an orbital (i.e., band) in the surface, and into or out of an orbital in the adsorbate. If the symmetry of the orbitals in the surface match those in the adsorbate, then the electron transfer process will be symmetry-allowed. If not, it will be symmetry forbidden.

An interesting feature is that when one changes the arrangement of the atoms around a catalytic site, one also changes the symmetry of the surface orbitals in the neighborhood of the site. Thus, a given elementary reaction can be symmetry-allowed at one site on the catalyst surface and symmetry-forbidden at a different site. This should result in a change in the reaction rate from site to site. Clearly, symmetry is not the only effect, and it might only be a small effect. However, if it is a large effect, then one could use an analysis of orbital symmetry to identify sites with unusual properties for further study.

The work here considers NO decomposition on platinum. A detailed analysis of the effects orbital symmetry on this reaction has been given previously (*16*). Basically when the reaction $NO_{(ad)} \rightarrow N_{(ad)} + O_{(ad)}$, occurs, electrons are transferred from the σ and π bonds in the NO to the metal (M) and from the metal to the σ^* and π^* orbitals in the NO. The $\sigma \rightarrow$ M and $\pi \rightarrow$ M transfers are symmetry allowed on all of the faces of platinum considered previously, but there are symmetry constraints on the M $\rightarrow \sigma^*$ and M $\rightarrow \sigma^*$ transitions. The π^*'s are antisymmetric around a plane through the molecular axis. Thus the M $\rightarrow \pi^*$ transition requires an antisymmetric orbital in the surface. However, all of the exposed orbitals on Pt(111) and Pt(110) are symmetric about the principal axes. Hence the elementary reaction $NO_{(ad)} \rightarrow N_{(ad)} + O_{(ad)}$ is symmetry-forbidden on Pt(111) and Pt(110). There are antisymmetric orbitals on Pt(100). However, the arrangement of the orbitals in the surface is such that the M $\rightarrow \sigma^*$ transition is partially forbidden. A similar analysis shows that the reaction is also partially or totally forbidden on all of the stepped surfaces considered previously, but there are some special stepped surfaces, such as Pt(410), where the orbitals at the step happen to line up properly so that the reaction is symmetry-allowed.

It is not known whether orbital symmetry effects are important to reactions on solid surfaces; however if they are, Pt(410) should be unusually active for NO decomposition. The purpose here is to test this idea using TPD.

EXPERIMENTAL METHODS

The data were taken in a vacuum system described previously (*17*). Briefly, the system was of standard design and had a base pressure below the X-ray limit of the ion gauge ($P < 2 \times 10^{-11}$ Torr). Partial pressures were measured with a Riber QX-100 mass spectrometer. Dosing of the samples was accomplished by either dosing from the ambient gases, or by orienting the sample so that it was 40 mm away from a tube fitted with a glass capillary array. The later procedure produced an increased dose at the front of the crystal. Calibration of the increased doses was accomplished by comparing ambient gas spectra to those taken with the capillary array.

Two different platinum single crystals were used in this study; one purchased from MRC and the other purchased from Metron. Each was aligned to within 0.5° of the (410) using Laue back reflection. The crystals were then cut by electrical discharge, producing oval samples of 8 × 6 × 1 mm. The samples were mechanically pol-

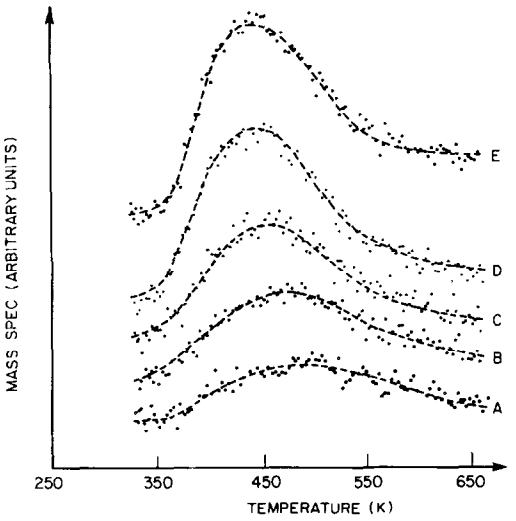

FIG. 1. Mass 28 (nitrogen) thermal desorption spectrum development with increasing NO exposure (Langmuirs): (A) 0.12 NO, (B) 0.20 NO, (C) 0.32 NO, (D) 0.8 NO, (E) 3.2 NO.

ished on both sides with final polishing done using 0.05-μm alumina. Prior to mounting the sample in the vacuum system, each sample was rinsed with dilute nitric acid. Auger analysis revealed that, at this point, the major surface impurities were carbon and oxygen. The crystals were then mounted in the vacuum chamber. Final cleaning was accomplished by heating briefly in oxygen, sputtering, then annealing in vacuum. The MRC crystal showed a buildup of calcium and silicon during the annealing cycle. However, no calcium or silicon was detected with the Metron single crystal (it was special ordered so that it was low in calcium and silicon). Both samples gave similar TPD spectra. However, all of the results presented here were taken with the Metron single crystal.

Each sample was supported in the vacuum system by two 1-mm tantalum wires. The sample was heated by electron bombardment in some of the runs and resistance heating in others. Electron bombardment gave a large Electron Stimulated Desorption (ESD) peak, so most of the data here were taken with resistance heating. The sample's temperature was monitored by a Chromel–Alumel thermocouple spot welded to the edge of the crystal. Data acquisition, and control of the heating rate were done by an LSI-11 minicomputer. Linear heating rates of 8 to 120°K/s reproducible to 0.5°K/s were possible. The thermocouple voltage and mass spectrometer output were stored in a binary file. The peak areas were integrated numerically.

RESULTS

Flash of an NO-covered Pt(410) crystal yields a nitrogen peak in the range of 400–500°K, and an oxygen peak above 900°K. In some of the runs, a small nitric oxide peak was seen at 380–500°K.

Figure 1 shows how the nitrogen peak varies with increasing exposure. At low exposures, a smooth, fairly symmetric featureless peak with a maximum at 486°K, is seen. Increasing exposure results in an increase in peak intensity and a decrease in peak temperature. The peak saturates at 3.2 Langmuirs, at which point the peak maximum lies at 439°K.

Figure 2 shows a plot of the NO peak taken under conditions similar to those in Fig. 1. There is a two peak structure, with a main peak at 410°K, and a smaller peak at about 480°K and an initial transient due to desorption from the heated support wires. The absolute intensity of the largest feature is only 15% of that of the N_2 peak. At a heating rate of 25°K/s one calculates a per-

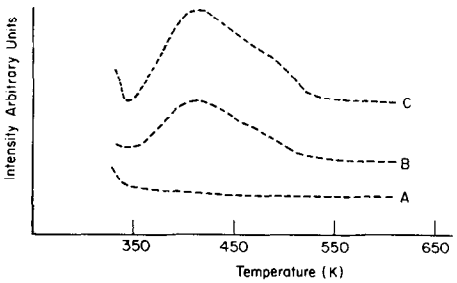

FIG. 2. Mass 30 (nitric oxide) TDS peak development with increasing NO exposure (Langmuirs): (A) 0.15 NO, (B) 1.5 NO, (C) 3.2 NO. The sample used for this data was polished on both faces but the edges were never polished or aligned. Other preparation procedures gave different results. See the text for details.

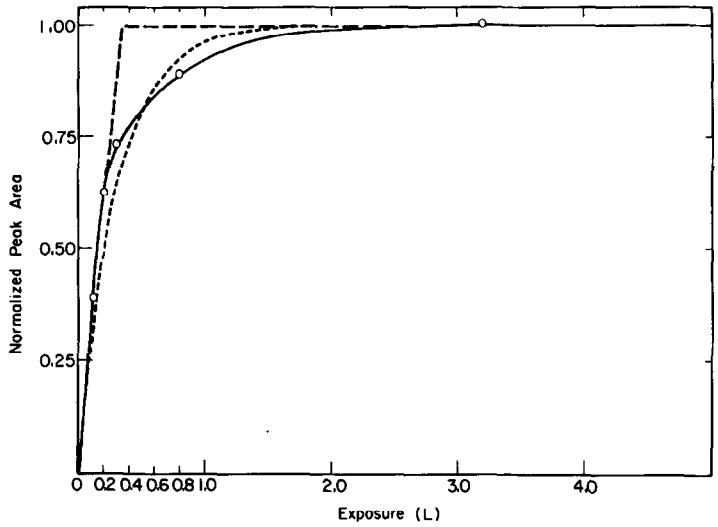

FIG. 3. Normalized coverage, θ (from nitrogen peak area) vs NO exposure in Langmuirs. (—○—) Experimental points, (---) constant sticking probability curve, and (· · · ·) Langmuir adsorption model.

cent dissociation, D, of 93% for this particular data set, where D is defined as in Eq. [1]. It has been found that the intensity of the NO peak varies significantly with some of the details of the experimental procedure. The data in Fig. 2 were taken with a crystal which was polished on the front and back, but the edges were never aligned or polished, and the back was never sputtered. Experiments were done with a crystal which was polished on only one side; there 70% of the NO dissociated and the 480°K peak was much larger than before. A series of runs were also done where a quartz shield was placed in front of the crystal, and a liquid nitrogen-cooled cold finger was placed behind the crystal; NO desorption was not detected in these runs. There was some interference with an ESD peak, however, so it would not have been possible to detect the 410°K NO peak if it was less than about 5% of the N_2 peak. It is argued, therefore, that most of the NO seen in Fig. 2 is a result of desorption from the edges and back of the crystal, with a multipeak structure arising because of different planes on the edges of the crystal. The data taken with the shield in front of the crystal shows that at room temperature more than 98% of the NO which adsorbs on Pt(410) dissociates before it desorbs.

Figure 3 shows a plot of the relative coverage, θ, calculated from the peak areas in Fig. 1, versus exposure. One can observe that the coverage increases linearly with exposure up to about 60% coverage, and then quickly saturates. The figure also shows a curve calculated for a Langmuir adsorption model (i.e., $S = S_0[1 - \theta]$) and a curve calculated assuming that the sticking probability is constant until all of the sites are filled. It appears that, for coverages below 75%, the curve calculated assuming a constant sticking probability fits the data much better than the curve calculated for the Langmuir model. Neither curve fits the data at higher coverages. This suggests that, indeed, the sticking probability is approximately constant up to 60–70% of saturation.

One can relate the initial slope in Fig. 3 to the saturation surface population, in molecules/cm^2, via a mass balance

$$n_0 = \frac{\left(\frac{v\rho}{P}\right)S_0}{\left(\frac{d\theta}{dL}\right)_0} \qquad (2)$$

where n_0 is the saturation surface population, v is the molecular velocity, ρ is the gas density at the dosing pressure P, θ is the relative coverage, L is the exposure, and S_0 is the initial sticking probability. Previous investigators have reported initial sticking probabilities in the range of 0.9–1.0 for NO adsorption on other faces of platinum (*5*). If it is assumed that the initial sticking probability of NO on Pt(410) is 0.95 then at room temperature the saturation surface population works out to be 5×10^{14} molecules/cm^2. Certainly there are many calibrations involved in getting this number so it could be subject to considerable error. However, we have also done similar measurements for CO adsorption on this surface and obtained $n_0 = 1.0 \times 10^{15}$ molecules/cm^2.

The data in Fig. 1 was compared to the predictions of a first-order and a second-order desorption model. The first-order model predicts asymmetric peaks which in the simplest analysis (i.e., the activation energy of desorption independent of coverage) have peak temperatures independent of coverage, while the second-order desorption model predicts symmetric peaks which shift to lower temperatures with increasing coverage. Clearly the data appear to be closer to second order than to first order.

Redhead has suggested a simple way to test for second-order desorption kinetics (*23*). One can show that for a second-order desorption process, the peak temperature, T_m, is related to the initial coverage, θ, by

$$\left(\frac{E_a}{RT_m^2}\right) = \left(\frac{\theta \nu n_0}{\beta}\right) \exp\left(-\frac{E_a}{RT_m}\right) \qquad (3)$$

where E_a is the activation energy of desorption, β is the heating rate, ν is the preexponential for desorption, and R is the gas law constant. Therefore a plot of $\ln(T_m^2\theta)$ versus $1/T_m$ should yield a straight line. Figure 4 shows such a plot. One can observe that the data scatter nicely around a line which implies that the data does indeed follow simple second-order kinetics.

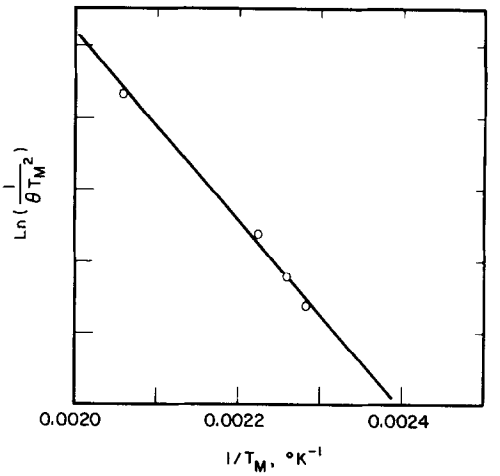

FIG. 4. A comparison of the data to the predictions of second-order kinetics in the way described in Redhead (*23*). θ was determined from integrated peak areas.

Redhead (*23*) also shows that one can measure the activation energy of desorption by varying the heating rate at constant exposure, and measuring how the peak temperature varies. A plot of $\ln(T_m^2/\beta)$ vs $1/T_m$ should yield a straight line with slope E_a/R and intercept $\ln(n_0\,\nu)$. Figure 5 shows such a plot for an exposure of 1.2 Langmuirs. Again, the data scatter around a straight line. From the slope of the plot one calculates an activation energy of 18 kcal/mol and a preexponential ($n_0\,\nu$) of 1.5×10^{12}/s or $\nu = 3 \times 10^{-2}$ cm^2/s.

Figure 5 is based exclusively on high coverage data. We also tried to do similar measurements at low coverages in an attempt to see if the activation energy of desorption varies with coverage. However, the low coverage peaks were very broad. There was considerable uncertainty in the peak temperatures, so the data on the plot were very scattered. Thus, it was difficult to reach any definite conclusions about the variation in the activation energy of desorption with coverage.

DISCUSSION

The results in the last section show that, indeed Pt(410) is unusually active for NO bond breaking, as predicted by our model.

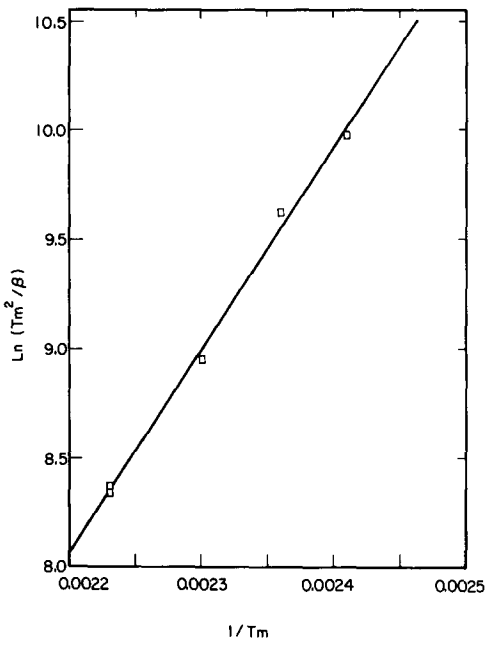

FIG. 5. The variation in the N_2 peak temperature (T_m) as heating rate (β) varied at a constant exposure of 1.2 Langmuirs NO.

Here we observe more than 98% dissociation of NO in the flash. We have done measurements with a polycrystalline sample and find 70% dissociation; Comrie *et al.* (*1*) report 75% dissociation with a similar polycrystalline sample. All of the platinum single crystals used by previous investigators dissociate 50% or less of the NO in a flash. Therefore it is concluded that Pt(410) has unusual bond breaking capabilities.

Other workers in our laboratory are conducting photoemission studies of NO adsorption on Pt(410). Their work (*26*) indicates that NO dissociates upon adsorption on Pt(410) at room temperature. The results in this paper are fully consistent with these other studies. Here it is found that the NO is nearly fully dissociated before it desorbs. The saturation coverage of NO corresponds roughly to one NO molecule for every two surface atoms while the CO saturation coverage corresponds to approximately one CO molecule for every surface atom. If we assume that the NO and CO compete for equivalent sites, as has been suggested previously (*27*), we conclude that the NO must take up two sites. Such a result provides additional evidence that NO is dissociatively adsorbed on Pt(410). Note that dissociative adsorption has not been seen below 420°K on any other previously studied face of platinum (*9, 10, 18*). This is additional evidence that Pt(410) has unusual NO bond breaking capabilities.

The adsorption data (i.e., Fig. 3) also seems to be quite consistent with previous work. It has been found that the sticking probability of CO and NO is independent of coverage up to about half coverage on a variety of metal surfaces (*5, 19, 20, 24*). The lack of variation in the sticking probability with coverage is normally explained by assuming that the adsorption occurs via a mobile precursor (*21*); King calls this an indirect adsorption process (*22*). It appears that we are also observing an indirect adsorption process. Evidently, what happens is that the NO adsorbs into a molecular state, and then "slowly" dissociates. CO adsorption on W(110) shows similar behavior above room temperature (*22*).

Our kinetics results show that nitrogen desorption follows second-order kinetics. This is just what one would expect if the recombination of two nitrogen atoms were rate controlling. The preexponential measured here is within normal limits. Therefore it is suggested that nitrogen recombination is rate controlling here. Note however that, on most other faces of platinum, the nitrogen desorption peak produced during the flash of a saturated NO layer behaves differently. For example, N_2 desorption from a polycrystalline or (100) sample follows apparent first-order desorption kinetics; these kinetics can also be explained with a second-order model, but one is required to assume an activation energy for desorption which varies significantly with coverage. The observation that the data here can be explained without invoking these complications suggests that there is some nontrivial difference between the processes on the (410) and those on other

faces. We suggest that there is a need to consider whether some step other than nitrogen recombination is rate determining during nitrogen desorption on other faces of platinum.

Another interesting observation is that the main N_2 desorption peak lies at higher temperature on the polycrystalline and (100) samples than it does on the (410). If one were to assume that heats of adsorption were proportional to activation energies of desorption (an assumption that clearly could be challenged) one would conclude that nitrogen is less strongly bound on Pt(410) than it is on other faces. Hence, based on energetics, one would expect Pt(410) to be less active than Pt(100) or polycrystalline platinum. The data show precisely the opposite. Clearly this is a special sample. It was chosen for the study because it was predicted to have sites of the right symmetry to break NO bonds. The orbital symmetry of NO and N_2 are almost the same. Thus according to our model the step sites on Pt(410) also have the right symmetry to form an N_2 molecule from two adsorbed nitrogen atoms. Our analysis suggests that there should be an extra barrier to N_2 desorption on most faces of platinum that is absent on Pt(410). While we do not have any direct evidence for this barrier, the observation that the activation energy of desorption of nitrogen is higher on the faces of platinum which are less active for NO bond breaking would suggest that some sort of barrier is present. This assertion also accounts for the observation that there does not appear to be two desorption modes (i.e., one from the terraces and another from the steps). We suggest that it is more efficient for the nitrogen molecules to diffuse to the steps, then desorb, rather than desorbing directly. Hence, one would only see one broad N_2 peak.

CONCLUSIONS

The results of this paper illustrate the potential utility of orbital symmetry conservation methods in identifying especially reactive sites on single crystal surfaces. Pt(410) is not a face that one would expect to be unusually active based on energetics. The (110), which has a lower average degree of saturation, is unreactive (*3*). Nitrogen bond energies, inferred from flash desorption peak temperatures, are lower on Pt(410) than on other platinum faces. Yet Pt(410) is much more adept at breaking NO bonds than any platinum face considered previously. Unlike other faces, the N_2 desorption kinetics follows a simple second-order rate law. We do not know whether symmetry-conservation methods will be as successful in identifying especially reactive sites for other reactions. However, the fact that they worked as well as they did here suggests that they deserve further study.

ACKNOWLEDGMENTS

This work was supported by the National Science Foundation under Grant CPE 80-12426. Equipment used in this work was provided by the NSF under Grant CPE 79-23249. This work made use of the University of Illinois, Center for the Microanalysis of Materials, which is supported as a national facility by the National Science Foundation under Grant DMR 80-20250.

REFERENCES

1. Comrie, C. M., Weinberg, W. H., and Lambert, R. M., *Surf. Sci.* **57,** 619 (1976).
2. Banholzer, W. F., M.S. thesis, University of Illinois, 1981.
3. Gorte, R. J., Schmidt, L. D., and Gland, J. L., *Surf. Sci.* **109,** 367 (1981).
4. Gland, J. L., and Sexton, B. A., *Surf. Sci.* **94,** 355 (1980).
5. Serri, J. A., Cardillo, M. J., and Becker, G. E., *J. Chem. Phys.* **77,** 2175 (1982).
6. Lin, T. H., and Somorjai, G. A., *Surf. Sci.* **107,** 573 (1981).
7. Campbell, C. T., Ertl, G., and Segner, J., *Surf. Sci.* **115,** 309 (1982).
8. Gorte, R. J., and Gland, J. L., *Surf. Sci.* **102,** 348 (1981).
9. Bonzel, H. P., and Pirug, G., *Surf. Sci.* **62,** 45 (1977).
10. Bonzel, H. P., and Fischer, T. E., *Surf. Sci.* **51,** 213 (1975).
11. Fischer, T. E., and Kelemen, S. R., *J. Catal.* **53,** 24 (1978).
12. Gland, J. L., *Surf. Sci.* **71,** 327 (1978).
13. Somorjai, G. A., Joyner, R. W., and Lang, B., *Proc. Roy. Soc. London Ser. A* **331,** 335 (1972).

14. Woodward, R. B., and Hoffmann, R., "The Conservation of Orbital Symmetry." Verlag Chemie, Weinheim, 1969.

15. Fukui, K., *Acc. Chem. Res.* **4,** 57 (1971).

16. Banholzer, W. F., Park, Y. O., Mak, K. M., and Masel, R. I., *Surf. Sci.* **128,** 176 (1983).

17. Horton, D. R., and Masel, R. I., *Surf. Sci.* **116,** 13 (1982).

18. Pirug, G., and Bonzel, H. P., *J. Catal.* **50,** 64 (1977).

19. Engel, T., *J. Chem. Phys.* **69,** 373 (1978).

20. McCabe, R. W., and Schmidt, L. D., *Surf. Sci.* **66,** 101 (1977).

21. Gorte, R., and Schmidt, L. D., *Surf. Sci.* **76,** 559 (1978).

22. King, D. A., *Surf. Sci.* **64,** 43 (1977).

23. Redhead, P. A., *Vacuum* **12,** 203 (1962).

24. Campuzano, J. C., Dus, R., and Greenler, R. G., *Surf. Sci.* **102,** 172 (1981).

25. Bonzel, H. P., Broden, G., and Pirug, G., *J. Catal.* **53,** 96 (1978).

26. Park, Y. O., Masel, R. I., Stolt, K., *Surf. Sci.* **131,** 385 (1983).

27. Lorimer, D., and Bell, A. T., *J. Catal.* **59,** 223 (1979).

28. Pearson, R. G., "Symmetry Rules for Chemical Reactions." Wiley, New York, 1981.